

Beam energy dependence of charge separation along the magnetic field in Au+Au collisions at RHIC

The STAR Collaboration

Local parity-odd domains are theorized to form inside the Quark-Gluon-Plasma (QGP) produced in high energy heavy ion collisions, and to manifest themselves as charge separation along the magnetic field via the chiral magnetic effect. Based on the approaches from previous STAR analyses of 200 GeV Au+Au collisions, we further this study into lower collision energies at $\sqrt{s_{NN}} = 7.7 - 62.4$ GeV. The signal gradually changes with decreased beam energy, and tends to diminish at 7.7 GeV. The beam energy dependency of the \mathcal{P} -even background is also discussed.

PACS numbers: 25.75.Ld

The strong interaction is parity even at vanishing temperature and isospin density [1], but parity could be violated locally in microscopic domains in QCD at finite temperature as a consequence of topologically non-trivial configurations of gauge fields [2, 3]. The Relativistic Heavy Ion Collider (RHIC) provide a good opportunity to study such parity-odd (\mathcal{P} -odd) domains, where the local imbalance of chirality results from the interplay of these topological configurations with the hot, dense and deconfined Quark-Gluon-Plasma (QGP) created in the heavy ion collisions

The \mathcal{P} -odd domains can be manifested via the chiral magnetic effect (CME). In heavy ion collisions, energetic spectator protons produce a strong magnetic field peaking around $eB \approx m_\pi^2$ [4], illustrated in Fig. 1. The strong magnetic field, coupled with the chiral asymmetry in the \mathcal{P} -odd domains, induces the electric charge separation along the direction of the magnetic field [4–9]. Based on data from STAR [10–12] and PHENIX [13, 14] Collaborations at RHIC and ALICE [15] at LHC, pertinent charge-separation fluctuations were experimentally observed, possibly providing an evidence for the CME. This interpretation is still under intense discussion, see e.g. [16, 17] and references therein.

Experimentally the fluctuations of charge separation are measured along the axis of the magnetic field, perpendicular to the reaction plane (containing the impact parameter and the beam momenta), with a three-point correlator, $\gamma \equiv \langle \cos(\phi_1 + \phi_2 - 2\Psi_{RP}) \rangle$ [18]. Here ϕ and Ψ_{RP} denote the azimuthal angles of a particle and the reaction plane, respectively. In practice, we approximate the reaction plane with the “event plane” (Ψ_{EP}) reconstructed with measured particles, and correct the measurement for the finite event plane resolution [10–12].

This Letter carries out the γ measurements of charged particles with Au+Au samples of 8M events at 62.4 GeV (2005), 100M at 39 GeV (2010), 46M at 27 GeV (2011), 20M at 19.6 GeV (2011), 10M at 11.5 GeV (2010) and 4M at 7.7 GeV (2010). Events selected with a minimum bias trigger have been sorted into centrality classes based on

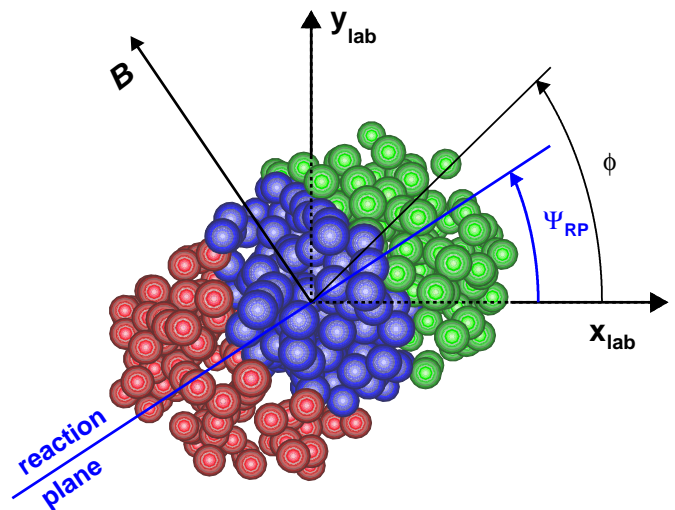


FIG. 1: (Color online) Schematic depiction of the transverse plane in a collision of two heavy ions (the left one emerging from and the right one going into the page). Particles are produced out of the overlap region. The azimuthal angles of the reaction plane and a produced particle used in the three-point correlator, γ , are depicted here.

charged particle multiplicity. Charged particle tracks in this analysis were reconstructed in the STAR Time Projection Chamber (TPC) [19], with a pseudorapidity cut $|\eta| < 1$ and a transverse momentum cut $0.15 < p_T < 2$ GeV/c. The centrality definition and track quality cuts are the same as in Ref. [20], unless otherwise specified. Only events within 40 cm of the center of the detector along the beam direction were selected for most data sets. This cut was 50 (70) cm for 11.5 (7.7) GeV collisions. To suppress events from collisions with the beam pipe (radius 3.95 cm), a cut on the radial position of the reconstructed primary vertex within 2 cm was applied. A cut on the distance of the closest approach to the primary vertex (DCA < 2 cm) was also applied to reduce the number of weak decay tracks or secondary interactions. The

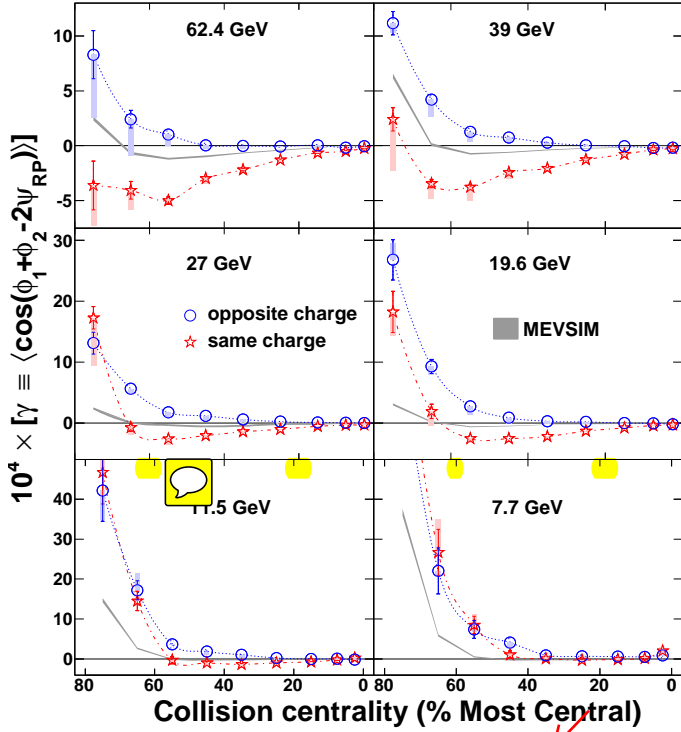


FIG. 2: (Color online) The three-point correlator as a function of centrality for Au+Au collisions at 7.7–62.4 GeV. Note that the vertical scales are different for different rows. The filled yellow boxes start from the central values, and ends with the results with the extra conditions of $\Delta p_T > 0.15$ GeV/c and $\Delta \eta > 0.15$ to suppress HBT+Coulomb effects (as discussed in the text).

experimental observables involved in the analysis have been corrected for the particle tracking efficiency.

In an event, charge separation along the magnetic field (perpendicular to the reaction plane) may be described phenomenologically by sine terms in the Fourier decomposition of the charged particle azimuthal distribution

$$\frac{dN_{\pm}}{d\phi} \propto 1 + 2v_1 \cos(\Delta\phi) + 2a_{\pm} \sin(\Delta\phi) + 2v_2 \cos(2\Delta\phi) + \dots \quad (1)$$

where $\Delta\phi = \phi - \Psi_{RP}$. Conventionally v_1 is called “directed flow” and v_2 “elliptic flow”, and they describe the collective motion of the produced particles [21]. The a_{\pm} parameters, $a_{-} = -a_{+}$, quantifies the \mathcal{P} -violating effect. The predicted spontaneous parity violation implies that the signs of a_{+} and a_{-} vary from event to event, leading to $\langle a_{+} \rangle = \langle a_{-} \rangle = 0$. In the expansion of the correlator, $\gamma = \langle \cos(\Delta\phi_1) \cos(\Delta\phi_2) - \sin(\Delta\phi_1) \sin(\Delta\phi_2) \rangle$, the second term contains the fluctuation $-\langle a_{\pm} a_{\pm} \rangle$, which may be non-zero when accumulated over particle pairs of separate charge combinations. The first term in the expansion provides a baseline unrelated to the magnetic field.

The reaction plane of a heavy-ion collision is not known a priori, and in practice it is approximated with the

event plane reconstructed from particle azimuthal distributions [21]. In this analysis, we exploited the large elliptic flow of charged hadrons produced at mid-rapidity

$$\Psi_{EP} = \frac{1}{2} \tan^{-1} \left[\frac{\sum \omega_i \sin(2\phi_i)}{\sum \omega_i \cos(2\phi_i)} \right], \quad (2)$$

where ω_i is a weight for each particle i in the sum [21]. The weight was chosen to be the p_T of the particle itself. Although the STAR TPC has good azimuthal symmetry, small acceptance effects in the calculation of the event plane azimuth were removed by the method of shifting [22]. The observed correlations were corrected for the event plane resolution, estimated with the correlation between two random sub-events (details in Ref. [21]).

The event plane thus obtained from the produced particles is also called “the participant plane” since it is subject to the event-by-event fluctuations of the initial participant nucleons [23]. A better approximation to the reaction plane could be obtained from the spectator neutron distributions detected in the STAR-ZDC-SMD [24]. This type of event plane utilizes the directed flow of spectator neutrons measured at very forward rapidity. As to the three-point correlator, measurements carried out with both types of event planes turned out to be consistent with each other [12]. Other systematic uncertainties were studied extensively in the previous publications on this subject [10, 11]. All were shown to be negligible compared with the uncertainty in determining the reaction plane. In this work, we only used the participant plane because the efficiency of ZDC-SMD becomes very low for low beam energies.

Figure 2 presents the opposite-charge (γ_{OS}) and same-charge (γ_{SS}) correlators for Au+Au collisions at $\sqrt{s_{NN}} = 7.7 - 62.4$ GeV as a function of centrality (0 means the most central collisions). In most cases, the ordering of γ_{OS} and γ_{SS} is the same as in Au+Au (Pb+Pb) collisions at higher energies [10–12, 15], manifesting extra charge-separation fluctuations perpendicular to the reaction plane. As a systematic check, the charge combinations of ++ and -- are always found to be consistent with each other (not shown here). With decreased beam energy, both γ_{OS} and γ_{SS} tend to rise up in peripheral collisions. This feature seems to be charge independent, and can be explained by momentum conservation and elliptic flow [12]. Momentum conservation forces all produced particles, regardless of charge, to separate from each other, while elliptic flow works in the opposite sense. For peripheral collisions, the multiplicity (N) is small, and momentum conservation dominates. The lower beam energy, the smaller N , and the higher γ_{OS} and γ_{SS} . For more central collisions where the multiplicity is large enough, this type of \mathcal{P} -even background can be estimated with $-v_2/N$ [12, 25]. MEVSIM is a Monte Carlo event generator developed for STAR simulations [26]. In Fig. 2, we also show the model calculations of MEVSIM with the implementation of v_2 and momentum conser-

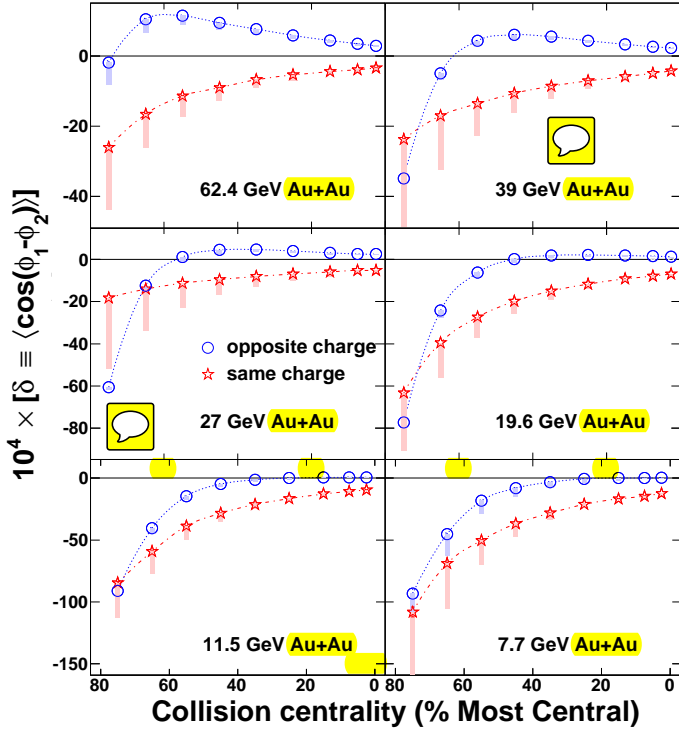


FIG. 3: (Color online) The two-particle correlation as a function of centrality for Au+Au collisions at 7.7–62.4 GeV. Note that the vertical scales are different for different rows. The filled boxes bear the same meaning as those in Fig. 2.

vation, which qualitatively describe the beam-energy dependency of the charge-independent background.

In view of the charge-independent background, the charge separation effect can be studied via the difference between γ_{OS} and γ_{SS} . ($\gamma_{OS} - \gamma_{SS}$) remains positive for all centralities down to the beam energy ~ 19.6 GeV, and the magnitudes decrease from peripheral to central collisions. Presumably this is partially owing to the reduced magnetic field and partially owing to the more severe dilution effect in more central collisions [11]. The difference approaches zero in peripheral collisions at lower energies, especially at 7.7 GeV, which is understandable in the picture of CME as the formation of QGP becomes less likely in peripheral collisions at low energies [27].

The systematic uncertainties of ($\gamma_{OS} - \gamma_{SS}$) due to the analysis cuts, the tracking efficiency and the event plane determination were estimated to be relative 10%, 5% and 10%, respectively. Overall, total systematic uncertainties are typically within 15%, except for the cases where ($\gamma_{OS} - \gamma_{SS}$) is close to zero. Another type of uncertainties is due to quantum interference (“HBT” effects) and final-state-interactions (Coulomb dominated) [12], which are most prominent for low relative momenta. To suppress the contributions from these effects, we applied the conditions of $\Delta p_T > 0.15$ GeV/c and $\Delta\eta > 0.15$ to the correlations, shown with filled boxes in Figs. 2, 3 and 4.



The interpretation of the γ results demands additional information on a two-particle correlation $\delta \equiv \langle \cos(\phi_1 - \phi_2) \rangle$, which also contains the fluctuation term $\langle a_{\pm} a_{\pm} \rangle$. Figure 3 shows δ as a function of centrality for Au+Au collisions at 7.7–62.4 GeV. In most cases, δ_{OS} is above δ_{SS} , indicating an overwhelming background over any possible CME effect. The background sources, if coupled with collective flow, will also contribute to γ . Taking this into account, one can express γ and δ in the following forms, where the unknown parameter κ , as argued in Ref. [28], is of the order of unity:

$$\gamma \equiv \langle \cos(\phi_1 + \phi_2 - 2\Psi_{RP}) \rangle = \kappa v_2 F - H \quad (3)$$

$$\delta \equiv \langle \cos(\phi_1 - \phi_2) \rangle = F + H, \quad (4)$$

where H and F are the CME and background contributions, respectively. In the discussion in Ref. [28] $\kappa = 1$, but it could deviate from unity owing to the finite detector acceptance and the theoretical uncertainties. We can solve for H ,

$$H^{\kappa} = (\kappa v_2 \delta - \gamma) / (1 + \kappa v_2). \quad (5)$$

Figure 4 shows $H_{SS} - H_{OS}$ as a function of beam energy for three centrality bins in Au+Au collisions. The default values (dotted curves) are from $H^{\kappa=1}$, and the solid (dash-dot) curves are obtained with $\kappa = 1.5$ ($\kappa = 2$). For comparison, the results for 10–60% Pb+Pb collisions at 2.76 TeV are also shown [15]. In the case of unity κ , ($H_{SS} - H_{OS}$) demonstrates a weak energy dependency above 19.6 GeV, and tends to diminish from 19.6 to 7.7 GeV, though the statistical errors are large for 7.7 GeV. This may be explained by the probable domination of hadronic interactions over partonic ones at low energies. With increased κ , ($H_{SS} - H_{OS}$) decreases for all beam energies and may even totally disappear in some case (e.g. with $\kappa \sim 2$ in 10–30% collisions). Provided better theoretical estimates of κ in future, a more conclusive result can be extracted from Fig. 4 with interpolation or extrapolation of the data.

In summary, a three-point correlation between two charged particles and the reaction plane has been carried out for Au+Au collisions at $\sqrt{s_{NN}} = 7.7$ –62.4 GeV. The general trend of separate correlations (γ_{OS} and γ_{SS}) as a function of centrality and beam energy can be qualitatively described by the model calculations of MEVSIM, indicating the \mathcal{P} -even background due to momentum conservation and collective flow. The charge separation along the magnetic field was studied via ($H_{SS} - H_{OS}$), which shows a weak energy dependency down to 19.6 GeV and then falls at lower energies. This is consistent with the picture of local parity violation and chiral magnetic effect when the hadronic phase plays an increased role with decreased energy. The results will be more conclusive in future if we could increase the statistics by ten times for the low energies and if we could better control the theoretical uncertainty due to κ .

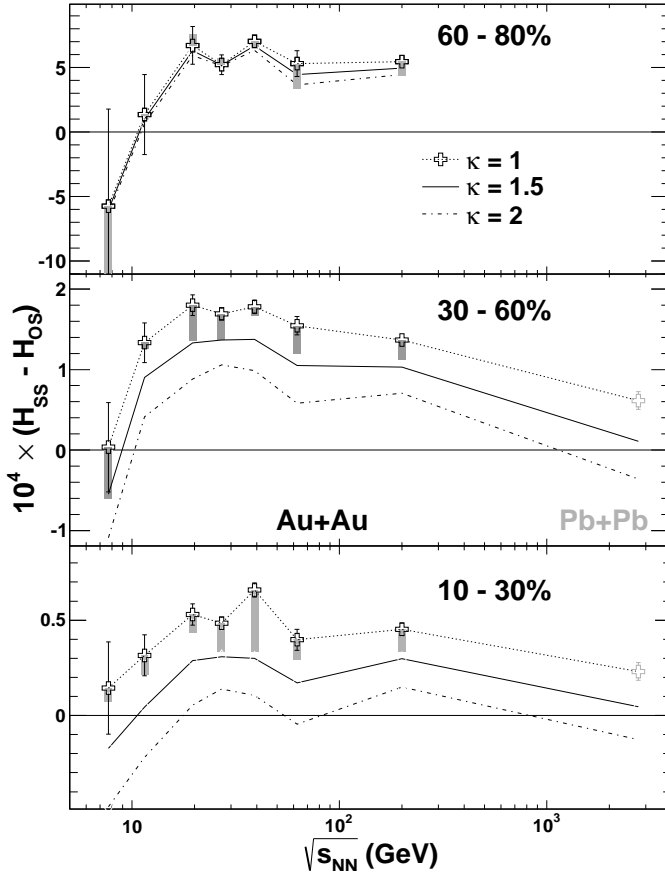


FIG. 4: (Color online) $H_{SS} - H_{OS}$, as a function of beam energy for three centrality bins in Au+Au collisions. The default values (dotted curves) are from $H^{\kappa=1}$, and the solid (dash-dot) curves are obtained with $\kappa = 1.5$ ($\kappa = 2$). For comparison, the results for Pb+Pb collisions at 2.76 TeV are also shown [15]. The systematic errors of the STAR data (filled boxes) bear the same meaning as those in Fig. 2.

We thank the RHIC Operations Group and RCF at BNL, the NERSC Center at LBNL and the Open Science Grid consortium for providing resources and support. This work was supported in part by the Observance of NP and HEP within the U.S. DOE Observation of Science, the U.S. NSF, the Sloan Foundation, CNRS/IN2P3, FAPESP CNPq of Brazil, Ministry of Ed. and Sci. of the Russian Federation, NNSFC, CAS, MoST, and MoE of China, GA and MSMT of the Czech Republic, FOM and NWO of the Netherlands, DAE, DST, and CSIR of India, Polish Ministry of Sci. and Higher Ed., National Research Foundation (NRF-

2012004024), Ministry of Sci., Ed. and Sports of the Rep. of Croatia, and RosAtom of Russia.

- [1] C. Vafa and E. Whitten, Phys. Rev. Lett. **53**, 535 (1984).
- [2] T. D. Lee, Phys. Rev. D **8**, 1226 (1973).
- [3] T. D. Lee and G. C. Wick, Phys. Rev. D **9**, 2291 (1974).
- [4] D. E. Kharzeev, L. D. McLerran and H. J. Warringa, Nucl. Phys. A **803** 227 (2008).
- [5] D. Kharzeev, Phys. Lett. B **633** 260 (2006).
- [6] D. Kharzeev and A. Zhitnitsky, Nucl. Phys. A **797** 67 (2007).
- [7] K. Fukushima, D. E. Kharzeev and H. J. Warringa, Phys. Rev. D **78** 074033 (2008).
- [8] D. E. Kharzeev, Annals Phys. **325** 205 (2010).
- [9] R. Gatto and M. Ruggieri, Phys. Rev. D **85** 054013 (2012).
- [10] B. I. Abelev *et al.* [STAR Collaboration], Phys. Rev. Lett. **103** 251601 (2009).
- [11] B. I. Abelev *et al.* [STAR Collaboration], Phys. Rev. C **81** 054908 (2010).
- [12] L. Adamczyk *et al.* [STAR Collaboration], Phys. Rev. C **88** 064911 (2013).
- [13] N. N. Ajitanand, S. Esumi, R. A. Lacey [PHENIX Collaboration], in: Proc. of the RBRC Workshops, vol. 96, 2010: "P- and CP-odd effects in hot and dense matter".
- [14] N. N. Ajitanand, R. A. Lacey, A. Taranenko and J. M. Alexander, Phys. Rev. C **83** 011901 (2011).
- [15] B. I. Abelev *et al.* [ALICE Collaboration], Phys. Rev. Lett. **110** 021301 (2013).
- [16] A. Bzdak, V. Koch and J. Liao, Phys. Rev. C **81** 031901 (2010); Phys. Rev. C **82** 054902 (2010).
- [17] D. E. Kharzeev, D. T. Son, Phys. Rev. Lett. **106** 062301 (2011).
- [18] S. Voloshin, Phys. Rev. C **70** 057901 (2004).
- [19] M. Anderson *et al.*, Nucl. Instr. Meth. A **499** 659 (2003).
- [20] L. Adamczyk *et al.* [STAR Collaboration], Phys. Rev. C **86** 54908 (2012).
- [21] A. M. Poskanzer and S. A. Voloshin, Phys. Rev. C **58** 1671 (1998).
- [22] J. Barrette *et al.*, Phys. Rev. C **56** 3254 (1997).
- [23] J. -Y. Ollitrault, A. M. Poskanzer and S. A. Voloshin, Phys. Rev. C **80** 014904 (2009).
- [24] B. I. Abelev *et al.* [STAR Collaboration], Phys. Rev. Lett. **101** 252301 (2008); and references therein.
- [25] A. Bzdak *et al.*, Phys. Rev. C **83** 014905 (2011).
- [26] R. L. Ray and R. S. Longacre, arXiv:nucl-ex/0008009 and private communication.
- [27] V.A. Okorokov, Int. J. Mod. Phys. E **22** 1350041 (2013).
- [28] A. Bzdak, V. Koch and J. Liao, Lect. Notes Phys. **871** 503 (2013) [[arXiv:1207.7327](https://arxiv.org/abs/1207.7327) [nucl-th]].